# uGMRT observation for HERA Calibration

Khandakar Md Asif Elahi, Samir Choudhuri, Nirupam Roy, Md Rashid, Phil Bull, Dharam Vir Lal

Radio Cosmology Conference, ICTS, 2025

# Motivation of this work

- **21-cm radiation from neutral hydrogen (HI):**
  An important tool to reveal the origin and the evolution of the first stars and galaxies of the Universe, and the nature of dark matter and dark energy.

- The 21-cm signal is buried under many orders of magnitude brighter emission from our Galaxy and other galaxies, collectively called the **foregrounds**

- It is necessary to have **an extremely high dynamic range calibration of the telescope**

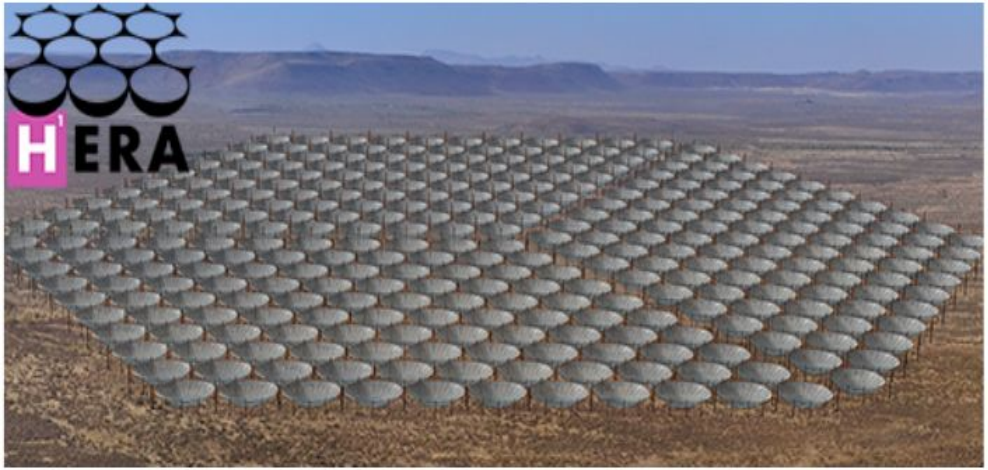

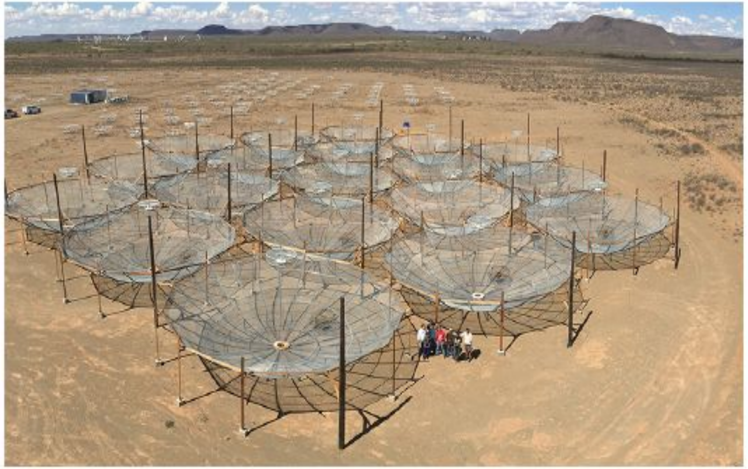

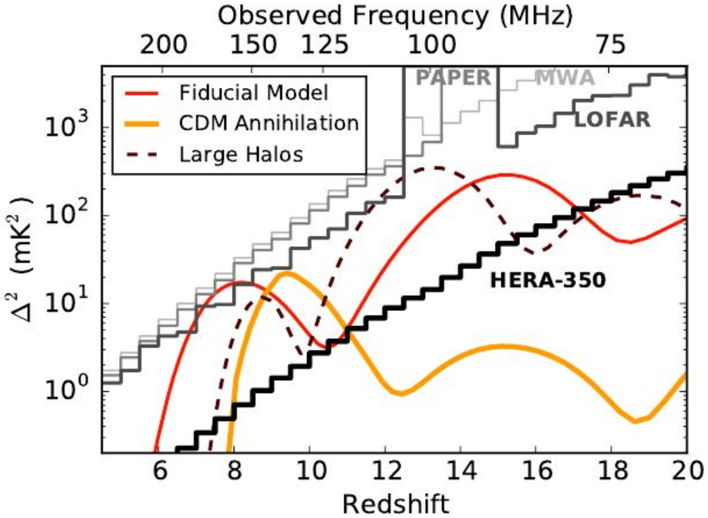
Observed Frequency (MHz)
200
150
125
100
75
PAPER
MWA
LOFAR
Fiducial Model
CDM Annihilation
Large Halos
HERA-350
$\Delta^2$ (mK$^2$)
$10^3$
$10^2$
$10^1$
$10^0$
6
8
10
12
14
16
18
20
Redshift

De Boer 17

# HERA calibration

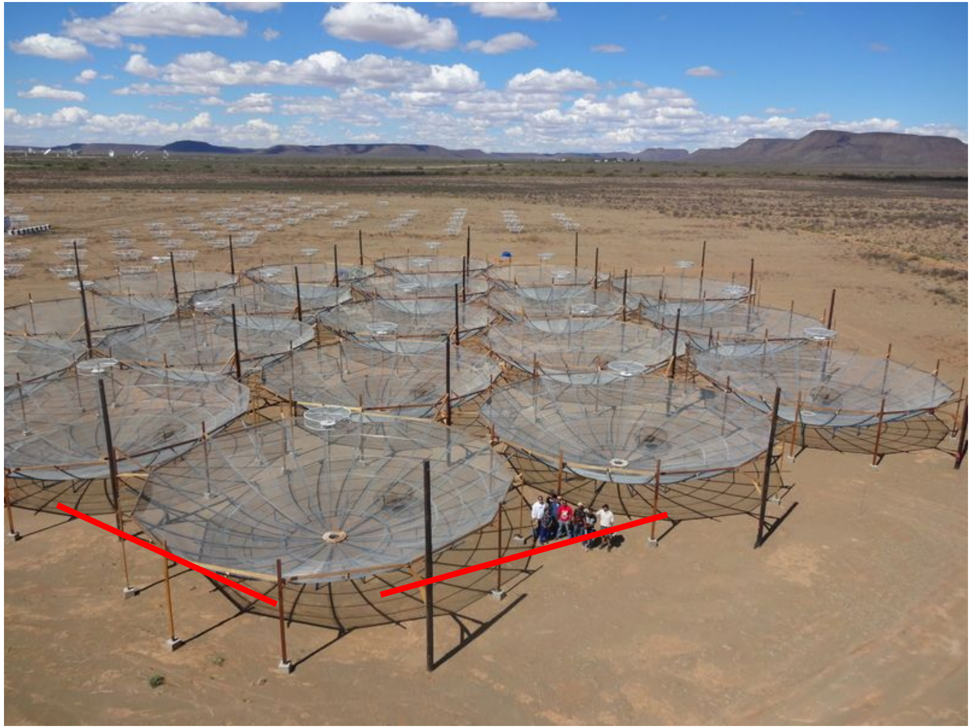

**Redundant calibration:**

$$V_{ij}^{\text{obs}} = g_i g_j^* V_{i-j} \qquad \langle V_{i-j} \rangle = V_{ij}^{\text{true}}$$

- Solve for the gains and unique visibilities simultaneously using the visibilities measured from **identical** baselines
- **No prior information about the sky or the instrument** other than the assumption that elements (baselines, beam) are identical.

**Absolute calibration:** fix the degeneracies

- Degenerate parameters: e.g., flux scale

$$g_i \rightarrow A g_i,\ V_{i-j} \rightarrow A^{-2} V_{i-j}$$

**Absolute calibration:** **Requires a sky-model that is**

- Complete
- Accurate in position
- Accurate measurements of spectral indices to reduce spectral errors

## HERA uses GLEAM catalogue

- 90% complete at 50 mJy
- 50% at 25 mJy
- angular resolution: ~2.5 arcmin at 154 MHz.

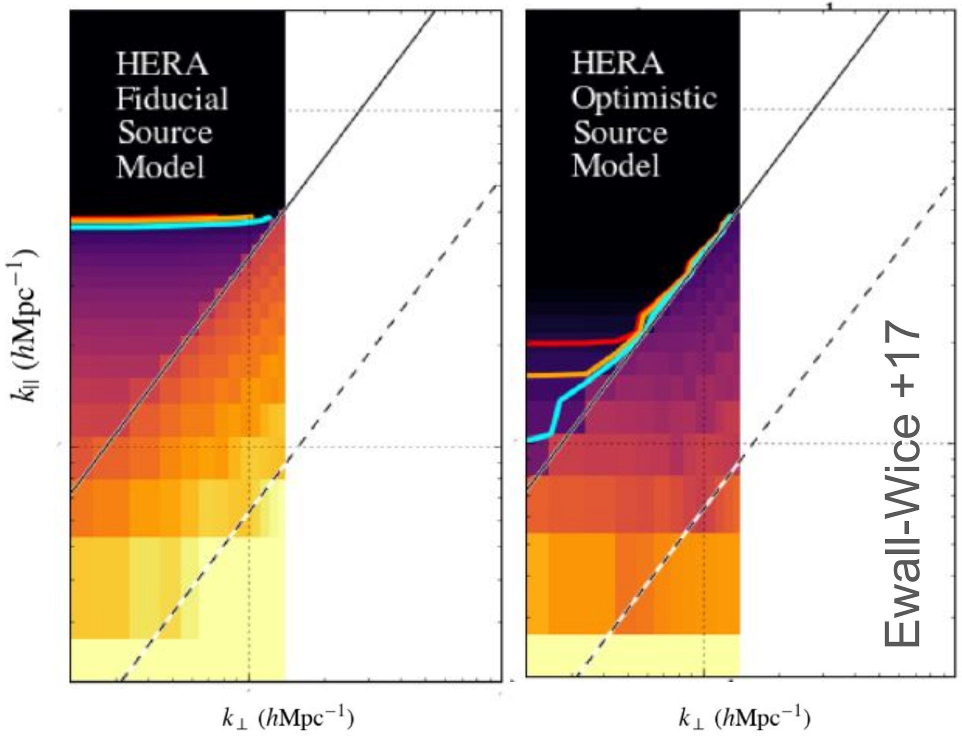


Ewall-Wice +17

# Motivation of this work

We plan to utilize the **high angular resolution** and **wide bandwidth** of ***uGMRT to improve the absolute calibration of the Hydrogen Epoch of Reionization Array (HERA)***,

Increase completeness at lower fluxes, detecting fainter sources

- **High-resolution**: identify more sources
- Increased accuracy in spectral index measurement using GWB data.

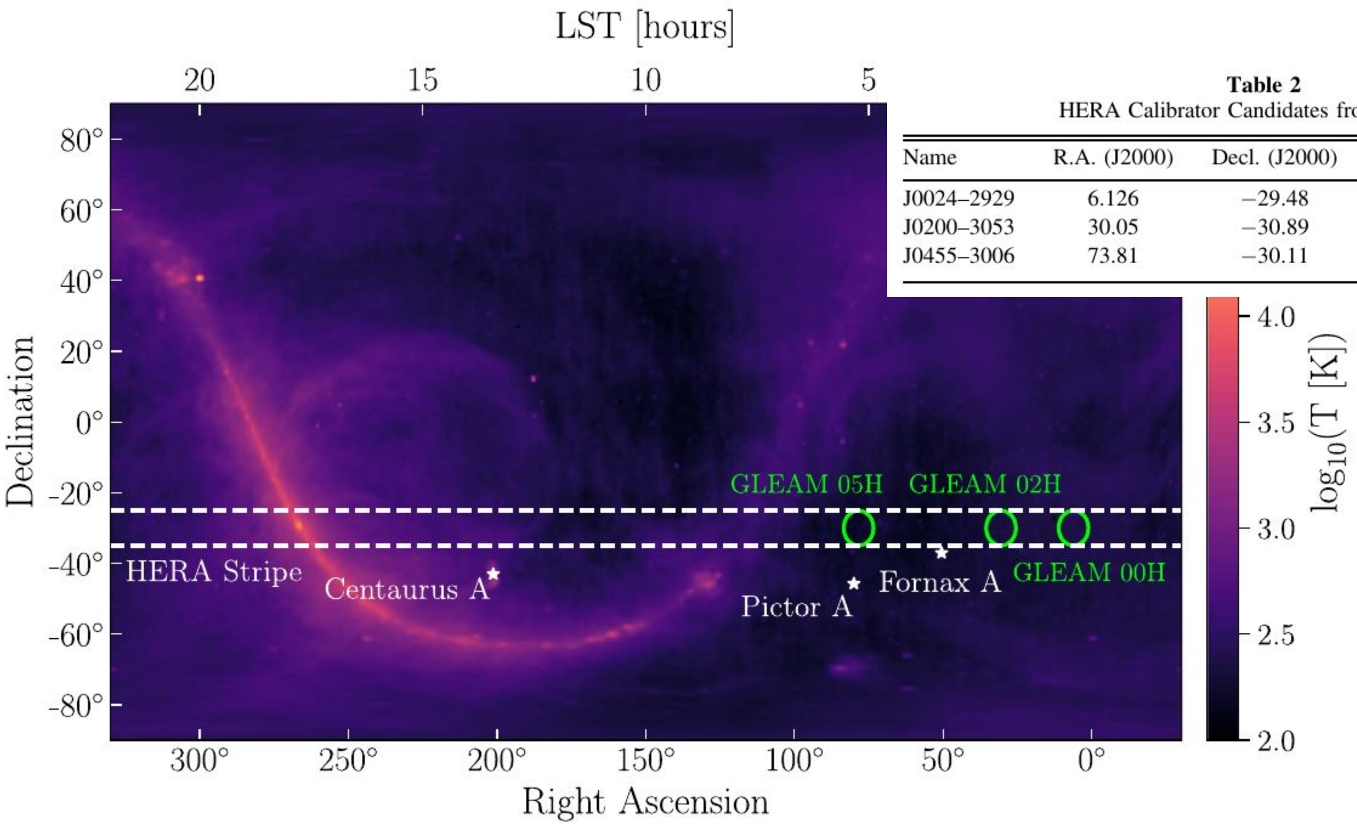


**Table 2**
HERA Calibrator Candidates from GLEAM

| Name | R.A. (J2000) | Decl. (J2000) | $S_{peak}$ | $S_{int}$ | $\alpha$ |
|---|---|---|---|---|---|
| J0024–2929 | 6.126 | −29.48 | 16.45 | 16.10 | −0.867 |
| J0200–3053 | 30.05 | −30.89 | 19.50 | 17.95 | −0.863 |
| J0455–3006 | 73.81 | −30.11 | 16.34 | 17.11 | −0.781 |

**Figure 3.** Radio sky at 150 MHz from the GSM (de Oliveira-Costa et al. 2008), showing the bright galactic and extragalactic foregrounds that stand in the way of cosmological 21 cm experiments. The HERA stripe is shown by white dashed lines centered at HERA's decl. of −30°.7 with a width of 10°, which is the FWHM of the primary beam at 150 MHz. The three fields identified as ideal calibration fields are shown by green circles, and some bright extended sources in the vicinity are marked by stars.

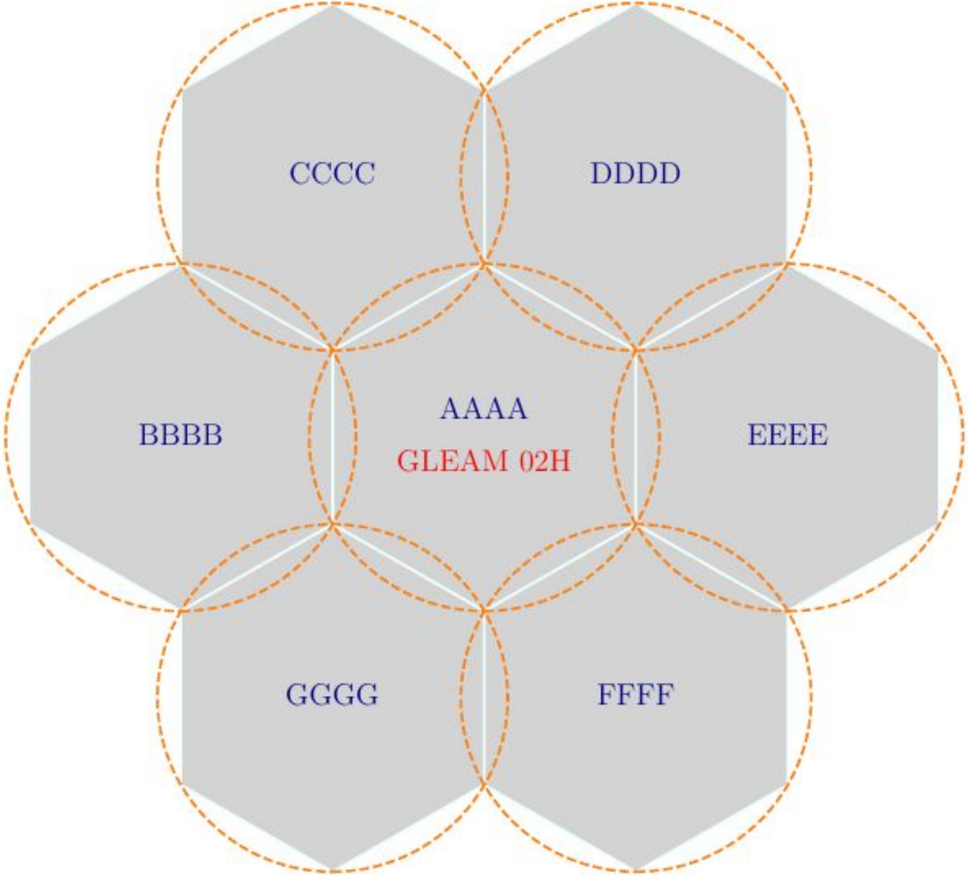


| Field Name | RA | Dec | Obs. Time (hours) |
|---|---|---|---|
| AAAA | $02^h\ 00^m\ 12.00^s$ | -30° 53′ 23.99″ | 1.77 |
| BBBB | $02^h\ 06^m\ 31.11^s$ | -30° 53′ 23.99″ | 1.77 |
| CCCC | $02^h\ 03^m\ 21.56^s$ | -29° 31′ 19.19″ | 1.77 |
| DDDD | $01^h\ 57^m\ 02.44^s$ | -29° 31′ 19.19″ | 1.77 |
| EEEE | $01^h\ 53^m\ 52.89^s$ | -30° 53′ 23.98″ | 1.77 |
| FFFF | $01^h\ 57^m\ 02.44^s$ | -32° 15′ 28.79″ | 1.77 |
| GGGG | $02^h\ 03^m\ 21.56^s$ | -32° 15′ 28.79″ | 1.77 |
| 3C 48 | $01^h\ 37^m\ 41.67^s$ | +33° 05′ 31.72″ | 2.32 |
| J0116-208 | $01^h\ 16^m\ 51.51^s$ | -20° 52′ 06.22″ | 2.22 |

**Observation**
uGMRT Band 2 (GSB)
Field: GLEAM 02H (RA, Dec: Table 1)
Observation: Strategy (Figure 1); Summary (Table 2)

**Table 2.** Observation Summary

| **Parameter** | **GSB** | **GWB** |
|---|---|---|
| Working antennas | 28-29 | 28-29 |
| Central Frequency | 147.4 MHz | |
| Bandwidth | 16.7 MHz | 120-250 MHz [8] |
| Frequency resolution | 65 kHz | 24.4 kHz |
| Integration time | 2 sec | 2 sec |
| Total Observation time | 17 hours | 17 hours |
| Overhead time | 3 hours | 3 hours |
| Calibrator time | 4.54 hours | 4.54 hours |
| On-source time | 12.4 hours | 12.4 hours |

**Calibration**

Direction independent and dependent using SPAM

Corrected for ionospheric effects

↓

**Imaging**

*Individual fields*: All nights combined data are imaged using AIPS (inside SPAM; see Table 1)

*Mosaic*: Primary beam corrected images are optimally added using ASTROPY (Summary: Table 3)

*Off-source rms of the mosaic*: 2 mJy/beam

Intema 2009, 2017

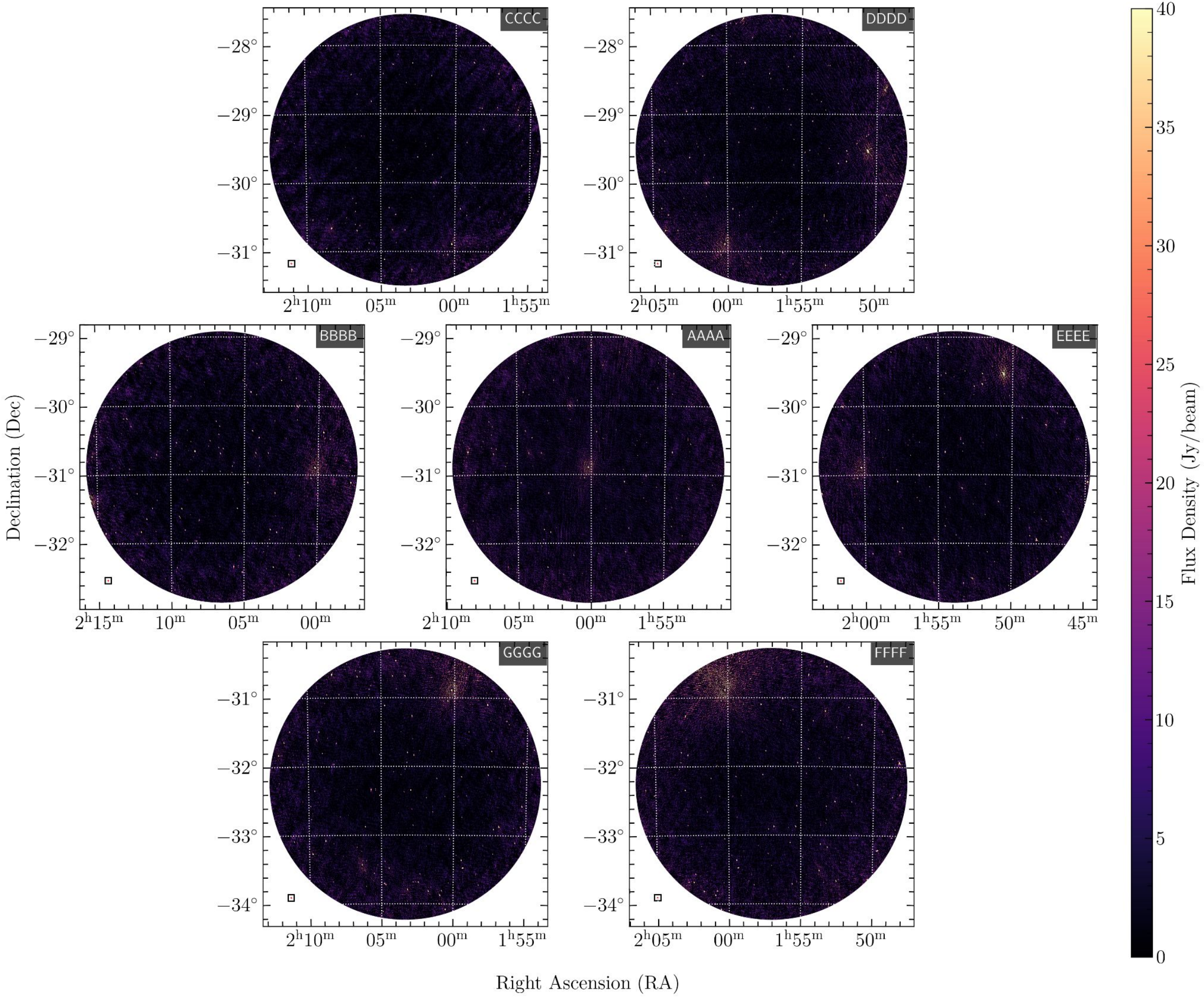

CCCC
DDDD
BBBB
AAAA
EEEE
GGGG
FFFF
Declination (Dec)
Right Ascension (RA)
Flux Density (Jy/beam)
−28°
−29°
−30°
−31°
−32°
−33°
−34°
2h15m
2h10m
2h05m
2h00m
10m
05m
00m
1h55m
50m
45m
0
5
10
15
20
25
30
35
40

| Field Name | Obs. Time (hours) | Flagging (%) | Theoretical rms (mJy) | Off-source rms (mJy/beam) | PSF (arcsec, PA) |
|---|---|---|---|---|---|
| AAAA | 1.77 | 54 | 0.44 | 4.906 | $29.7'' \times 14.8''$ (PA 23°) |
| BBBB | 1.77 | 30 | 0.35 | 2.853 | $39.3'' \times 14.6''$ (PA 23°) |
| CCCC | 1.77 | 30 | 0.35 | 2.577 | $32.7'' \times 14.9''$ (PA 12°) |
| DDDD | 1.77 | 30 | 0.35 | 2.549 | $30.0'' \times 15.2''$ (PA 13°) |
| EEEE | 1.77 | 29 | 0.35 | 2.862 | $31.9'' \times 14.8''$ (PA 22°) |
| FFFF | 1.77 | 29 | 0.35 | 3.379 | $32.4'' \times 16.7''$ (PA 25°) |
| GGGG | 1.77 | 30 | 0.35 | 2.694 | $34.9'' \times 15.5''$ (PA 15°) |

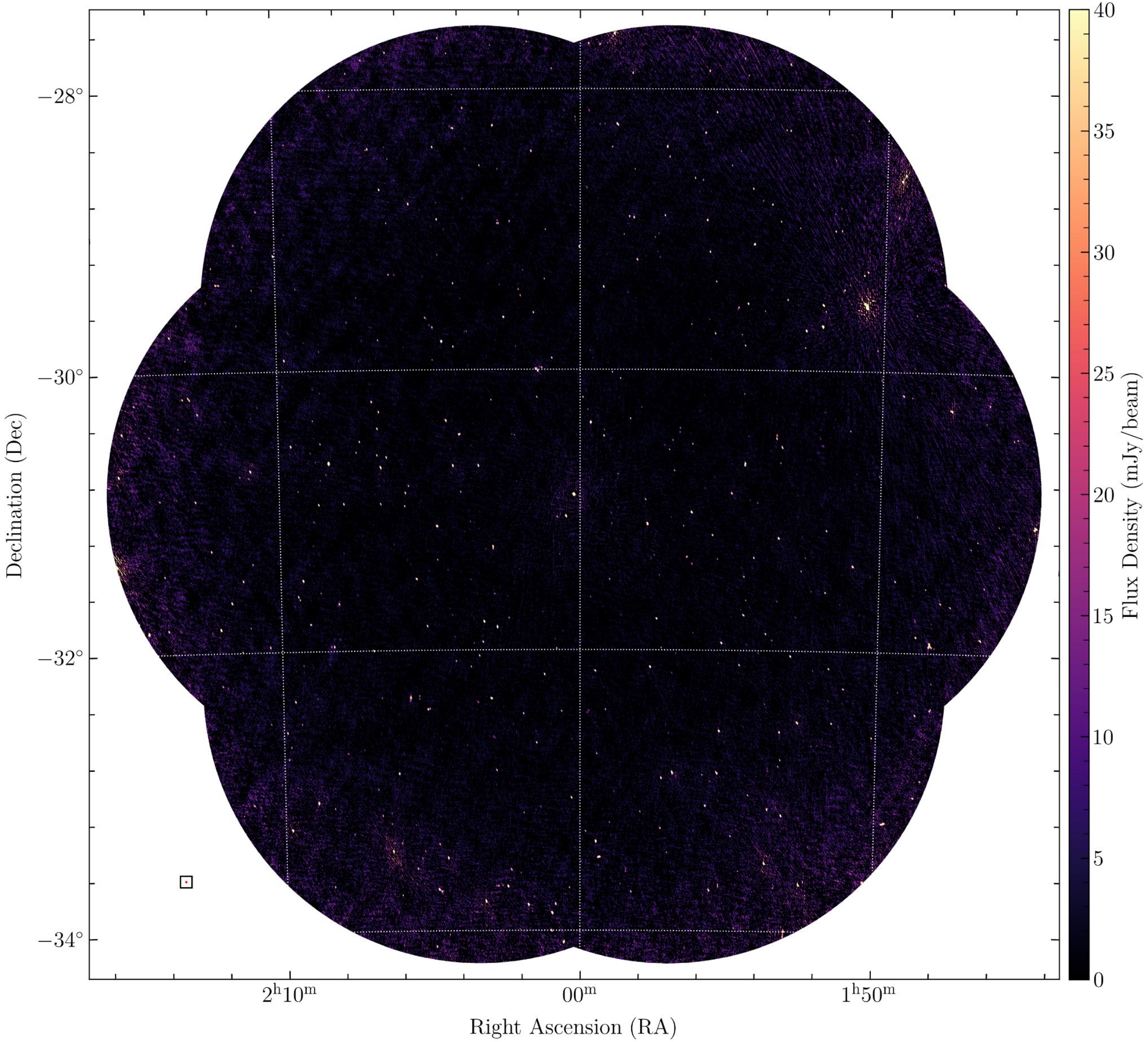


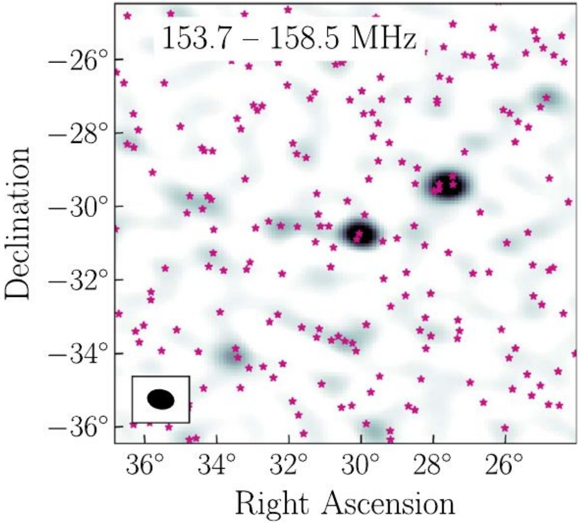


**Table 3.** Summary of the mosaic image

| Parameter | Value |
|---|---|
| Image size | 6077 × 6074 pixels |
| Pixel size | 4.10 × 4.10 arcsec |
| Off-source noise ($\sigma_{\rm rms}$) | 1.99 ± 0.18 mJy/beam |
| Peak flux density ($S_{\rm peak}$) | 12.04 Jy/beam |
| Minimum flux density ($S_{\rm min}$) | −0.13 Jy/beam |
| Dynamic range ($S_{\rm peak}/\sigma_{\rm rms}$) | ∼ 6000 |
| Synthesized beam (PSF) | 29.7 × 14.8 arcsec, PA = 23.66° |

## PKS 0157-31

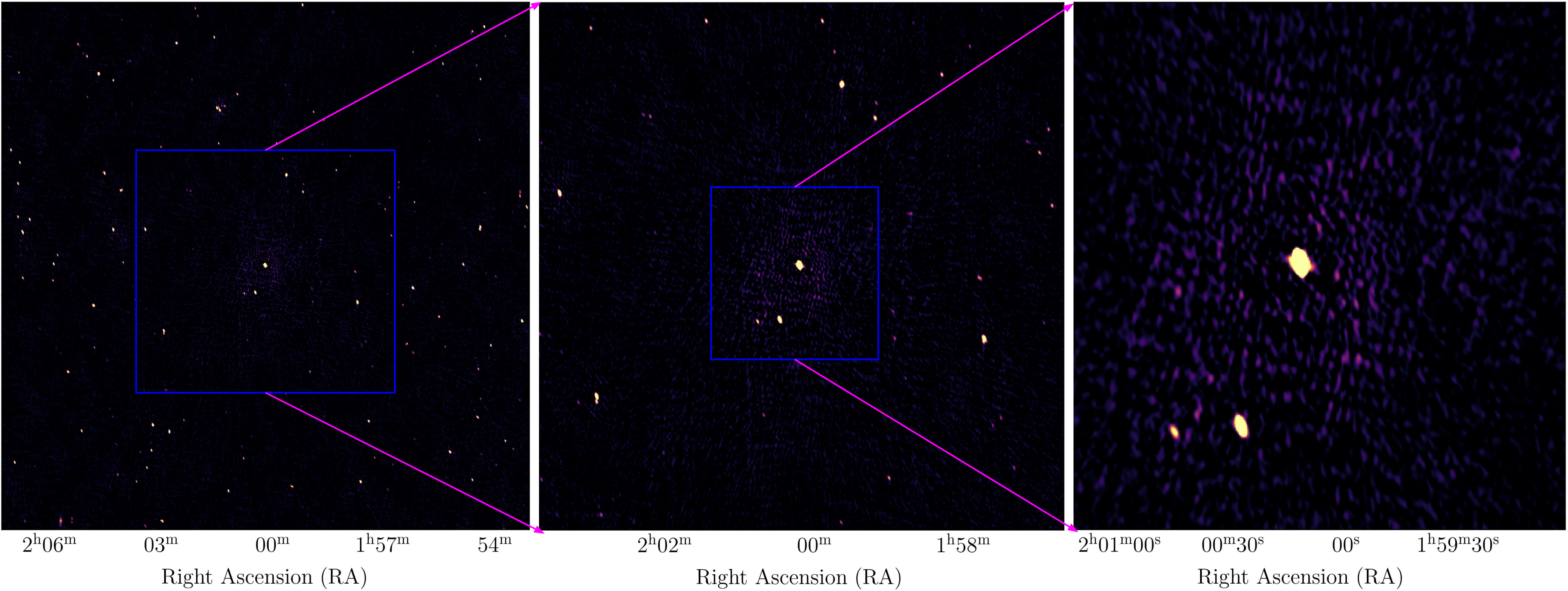

2h06m
03m
00m
1h57m
54m
Right Ascension (RA)
2h02m
00m
1h58m
Right Ascension (RA)
2h01m00s
00m30s
00s
1h59m30s
Right Ascension (RA)

## Source Catalogue
Using PyBDSF (Table 5)

| | Source_id | RA (deg) | DEC (deg) | Total_flux (Jy) | E_Total_flux (Jy) | Peak_flux (Jy/beam) | E_Peak_flux (Jy/beam) | Maj (arcsec) | Min (arcsec) | PA (deg) | Isl_rms (mJy) |
|---|---|---|---|---|---|---|---|---|---|---|---|
| PKS 0157-31 | 314 | 30.05 | -30.89 | 21.59 | 0.05 | 12.11 | 0.01 | 37.65 | 21.03 | 14.26 | 7.13 |
| ⇨ | 590 | 27.64 | -29.54 | 9.97 | 0.12 | 3.37 | 0.02 | 56.06 | 30.47 | 20.49 | 17.06 |
| ⇨ | 591 | 27.66 | -29.52 | 7.25 | 0.11 | 2.28 | 0.02 | 57.64 | 26.98 | 43.78 | 17.06 |
| | 1 | 33.86 | -31.36 | 5.22 | 0.07 | 2.77 | 0.02 | 38.38 | 21.46 | 22.53 | 23.74 |
| | 560 | 28.0 | -29.68 | 4.83 | 0.02 | 3.11 | 0.0 | 31.92 | 21.23 | 9.61 | 4.96 |
| | 79 | 32.08 | -30.66 | 3.26 | 0.02 | 0.94 | 0.0 | 46.26 | 27.54 | 173.01 | 3.27 |
| | 134 | 31.59 | -33.43 | 2.91 | 0.04 | 1.93 | 0.01 | 36.32 | 17.07 | 9.96 | 11.14 |
| | 612 | 27.38 | -28.64 | 2.78 | 0.05 | 1.72 | 0.02 | 30.37 | 21.63 | 6.95 | 15.56 |
| | 226 | 30.8 | -33.79 | 2.52 | 0.02 | 1.56 | 0.01 | 38.68 | 18.26 | 14.69 | 8.58 |
| | 365 | 29.72 | -27.6 | 2.11 | 0.05 | 1.4 | 0.01 | 38.29 | 18.68 | 6.59 | 12.64 |

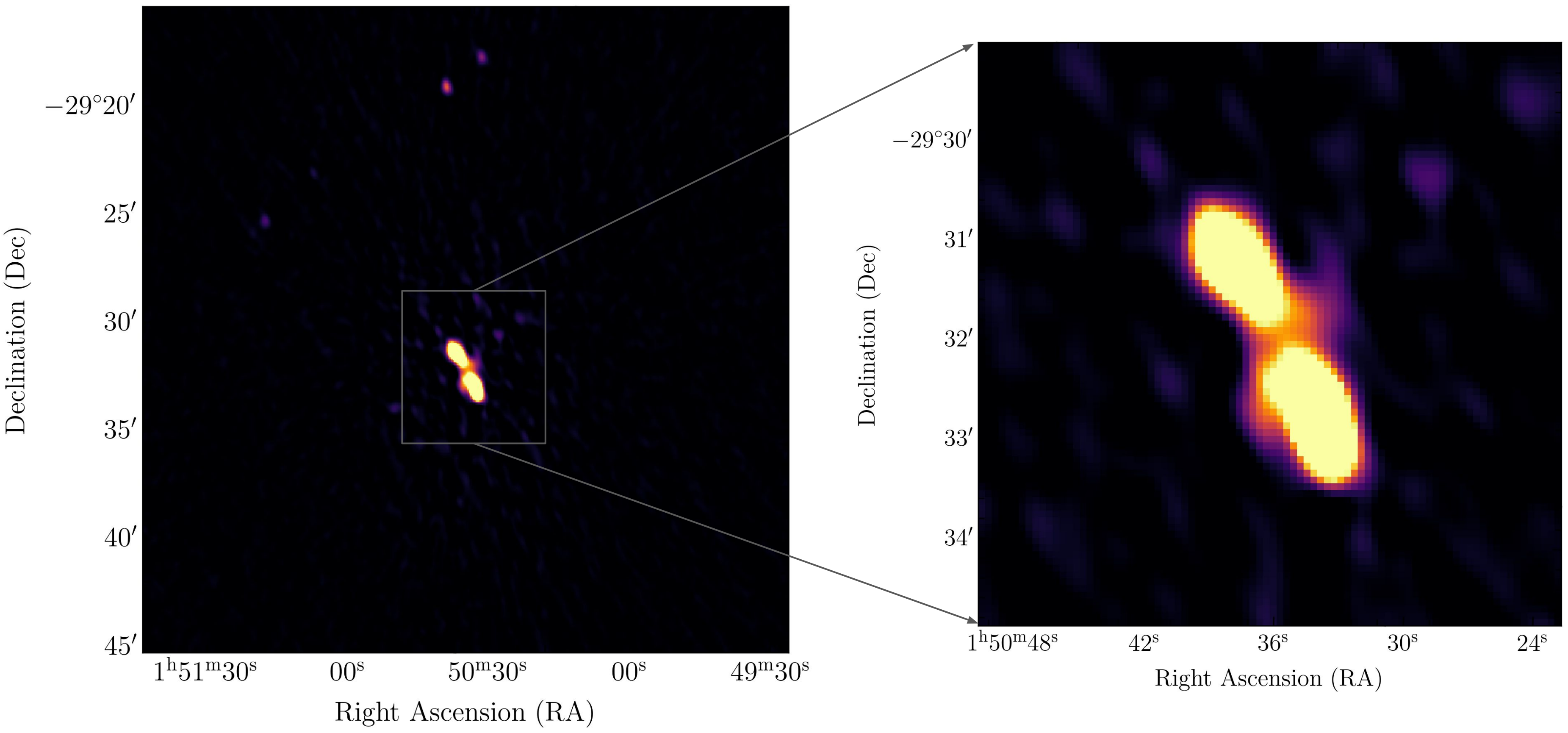

−29°20′
25′
30′
35′
40′
45′
Declination (Dec)
1h51m30s
00s
50m30s
00s
49m30s
Right Ascension (RA)
−29°30′
31′
32′
33′
34′
Declination (Dec)
1h50m48s
42s
36s
30s
24s
Right Ascension (RA)

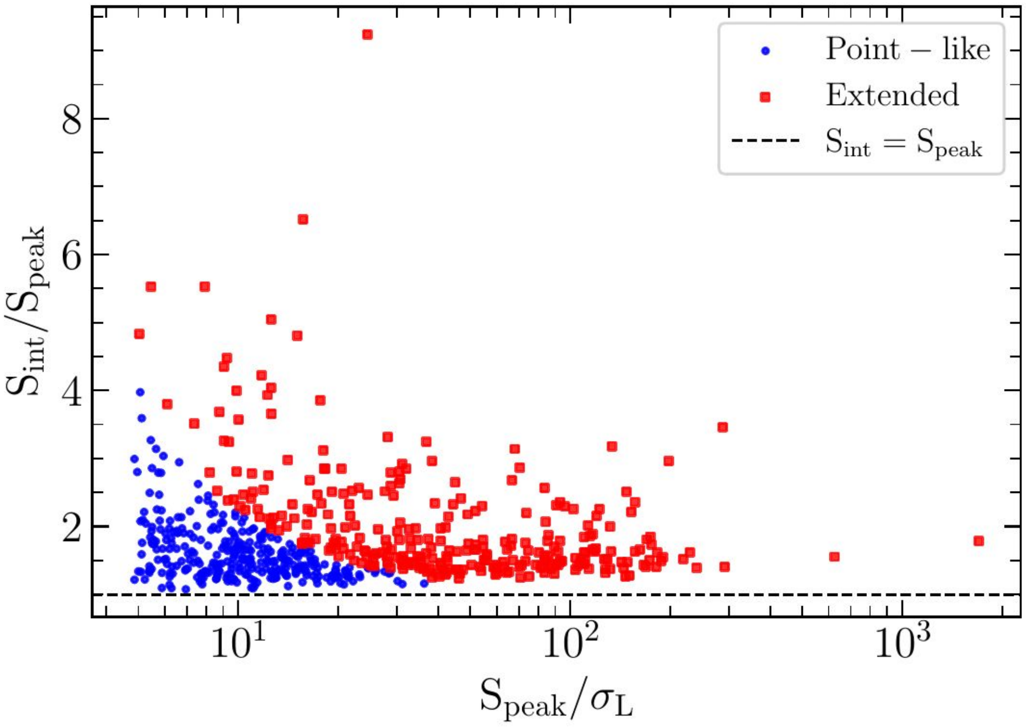


(Franzen et al. 2016)

$$R = \ln\left(\frac{S_{\rm int}}{S_{\rm peak}}\right) .$$

We obtain the uncertainty in $R$ using,

$$\sigma_R^2 = \left(\frac{\partial R}{\partial S_{\rm int}}\sigma_{S_{\rm int}}\right)^2 + \left(\frac{\partial R}{\partial S_{\rm peak}}\sigma_{S_{\rm peak}}\right)^2$$

$$= \left(\frac{\sigma_{S_{\rm int}}}{S_{\rm int}}\right)^2 + \left(\frac{\sigma_{S_{\rm peak}}}{S_{\rm peak}}\right)^2 .$$

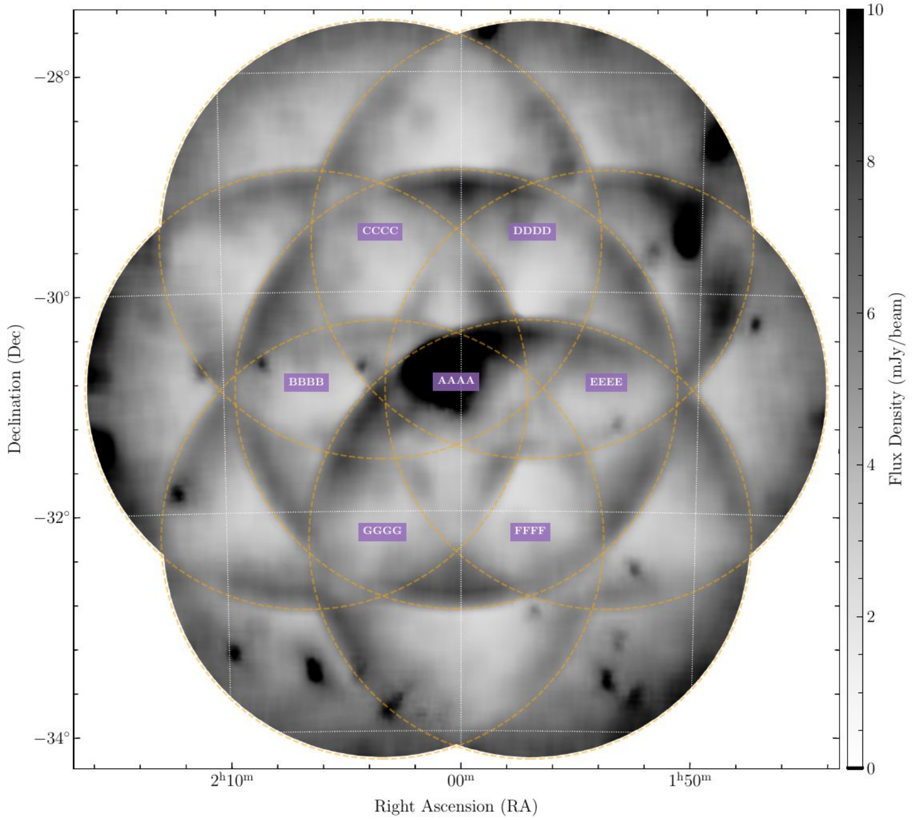


cumulative area of the mosaic which has an rms noise less than or equal to the corresponding rms level

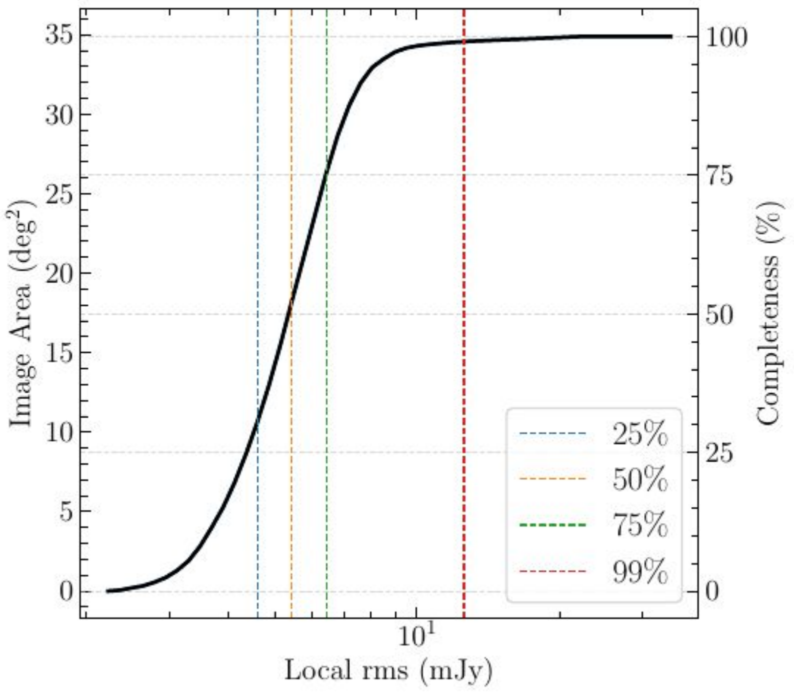


50% of the image area has an rms less than 5-6 mJy

**Cross-matching with Catalogues**
NVSS, TGSS, GLEAM, GLEAM-X
No positional offsets; flux accuracy within 10%

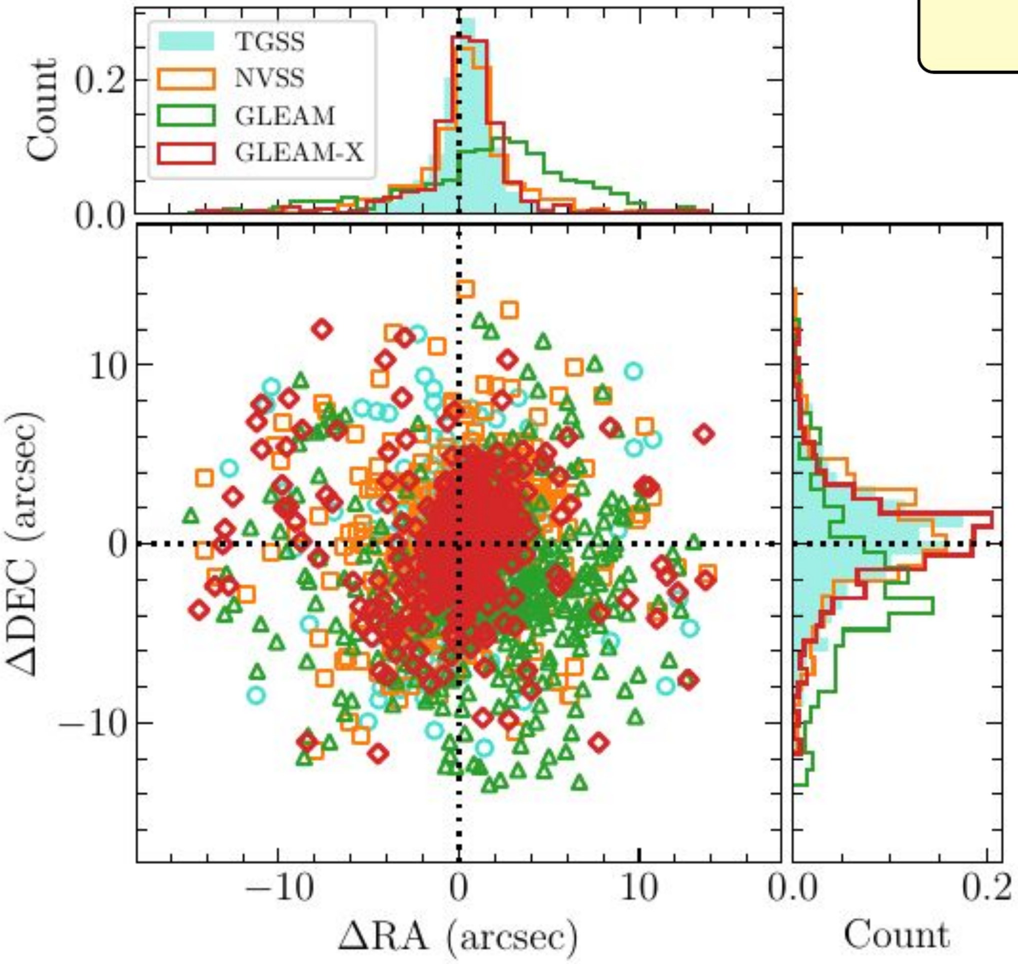

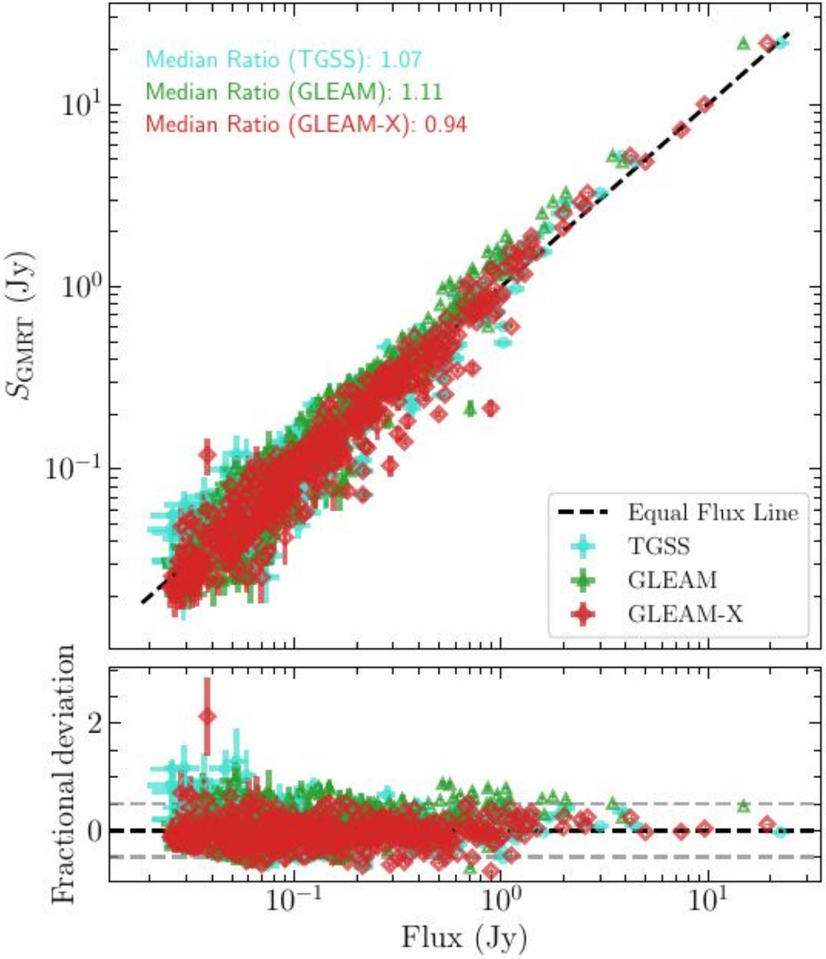


**Cross-matching with Catalogues**

NVSS, TGSS, GLEAM, GLEAM-X

No positional offsets; flux accuracy within 10%

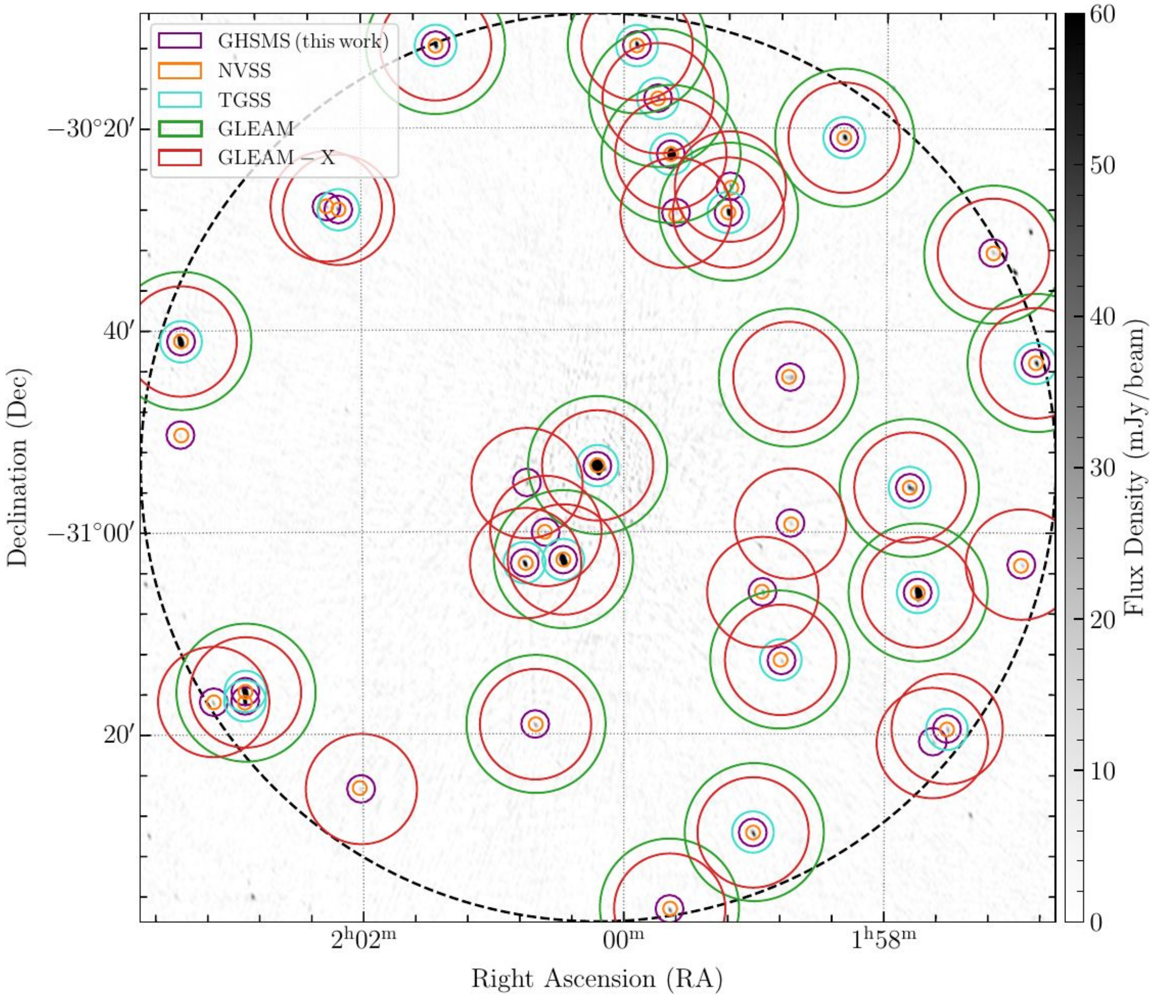

GHSMS (this work)
NVSS
TGSS
GLEAM
GLEAM − X
−30°20′
40′
−31°00′
20′
Declination (Dec)
2h02m
00m
1h58m
Right Ascension (RA)
60
50
40
30
20
10
0
Flux Density (mJy/beam)

**Spectral Index Distribution**

Using 1.4 GHz NVSS catalogue: $\alpha = -0.72^{-0.93}_{-0.50}$

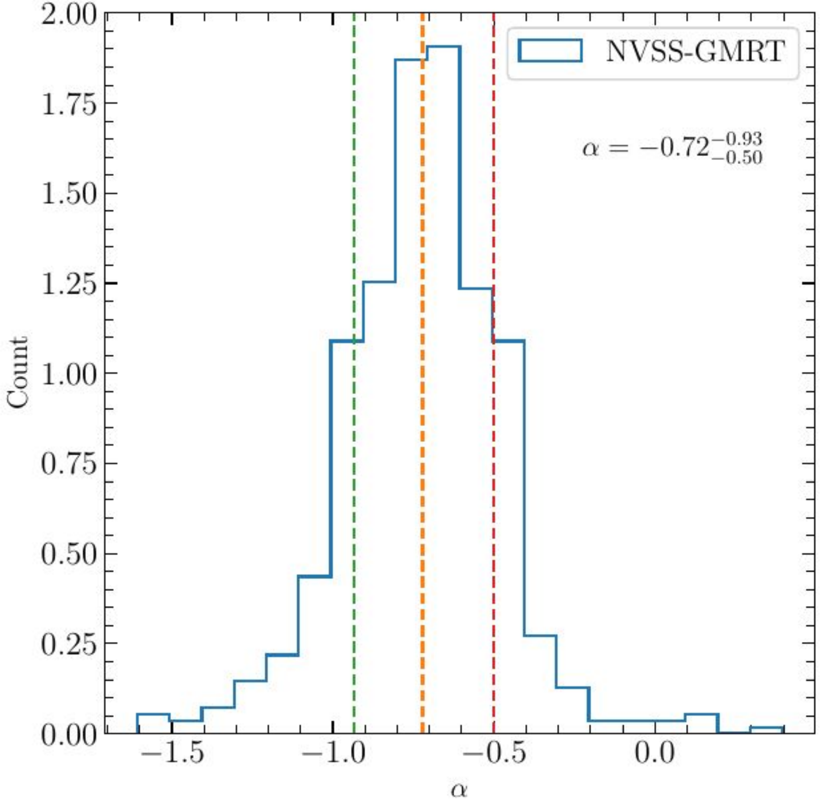

**Source Counts**

Computed Euclidean-normalized differential source counts

*Corrections*: FDR, Completeness

(includes Eddington and resolution bias)

Matched with GLEAM (Franzen et al. 2019) and LOFAR Surveys.

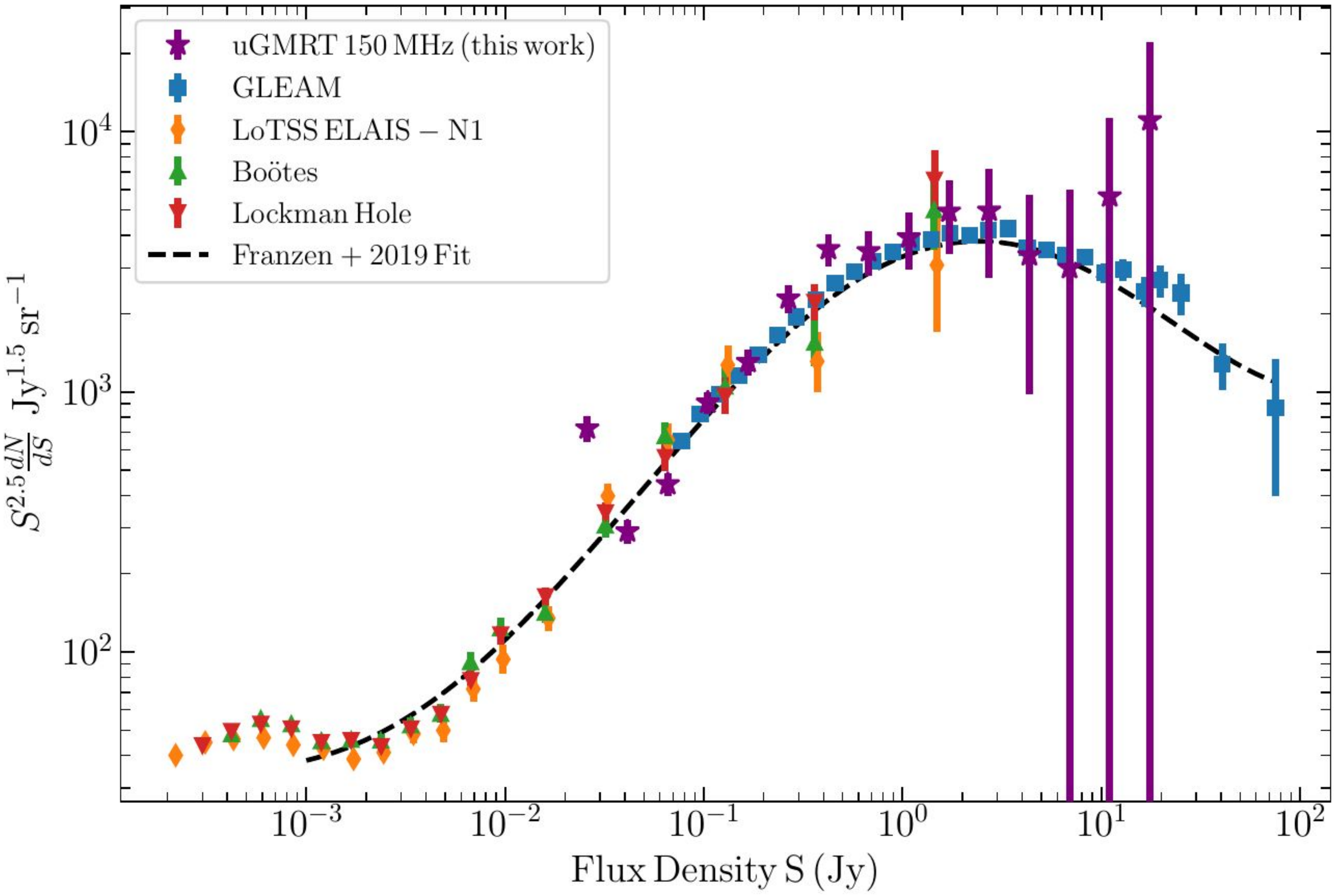

uGMRT 150 MHz (this work)
GLEAM
LoTSS ELAIS − N1
Boötes
Lockman Hole
Franzen + 2019 Fit
$S^{2.5}\frac{dN}{dS}$ Jy$^{1.5}$ sr$^{-1}$
$10^4$
$10^3$
$10^2$
$10^{-3}$
$10^{-2}$
$10^{-1}$
$10^0$
$10^1$
$10^2$
Flux Density S (Jy)

**Future Plan**

Deeper Image and source counts with GWB

In-band spectral index measurement

Galactic emission characterisation for improving -

HERA's short baseline calibration

Deeper observation of the GLEAM 02H field

Exploring two other calibration fields: GLEAM 00H, 05H

**Future Plan**

Deeper Image and source counts with GWB

In-band spectral index measurement

Galactic emission characterisation for improving -

HERA's short baseline calibration

Deeper observation of the GLEAM 02H field

Exploring two other calibration fields: GLEAM 00H, 05H

Thanks for your attention

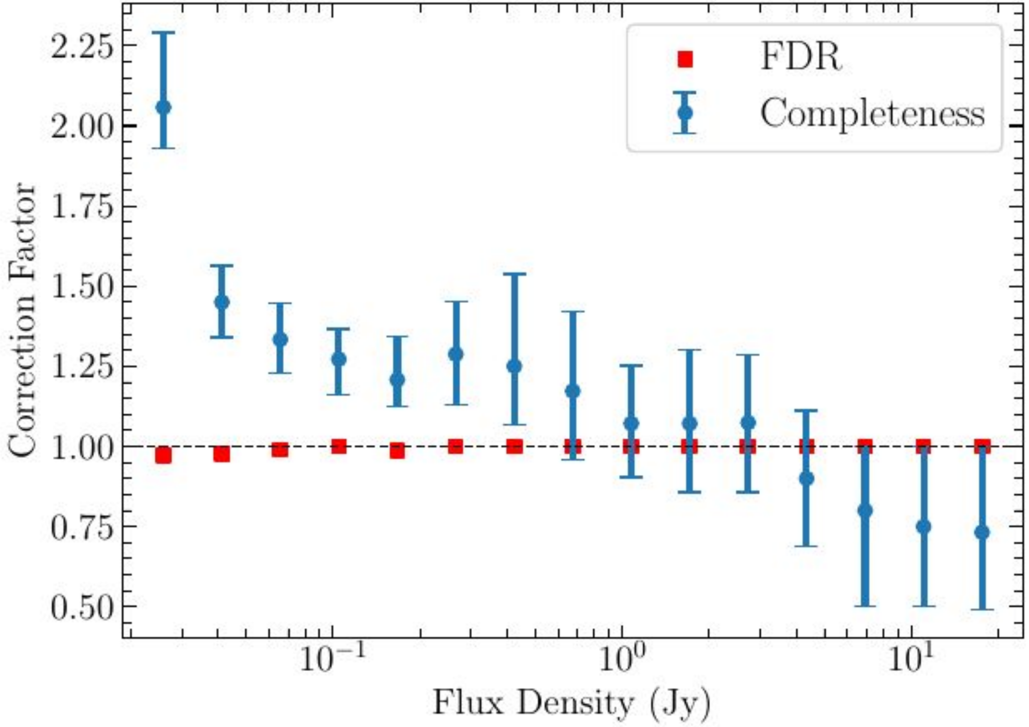

FDR
Completeness
2.25
2.00
1.75
1.50
1.25
1.00
0.75
0.50
Correction Factor
$10^{-1}$
$10^{0}$
$10^{1}$
Flux Density (Jy)

**Table 6.** The Euclidean normalised differential source counts $S^{2.5}\,dN/dS$ (Jy$^{3/2}$ sr$^{-1}$). The columns below correspond to the flux density bins $[S_i, S_f]$, the central value of the flux density bin $S$, bin widths ($\Delta S$), number of sources $N$, FDR correction ($C_{\rm fdr}$), completeness correction ($C_c$), visibility function, and Euclidean normalised source counts with errors. The visibility function $V(S)$ is written as $(A_{\rm eff}/A) \times 100\%$, where $A_{\rm eff}$ and $A$ are the effective and total image areas, respectively. The Euclidean normalised source count is computed as: $\left(\frac{N}{\Delta S \times A_{\rm eff}}\right) \times S^{2.5} \times C_{\rm tot}$, where $C_{\rm tot} = C_{\rm fdr} \times C_{\rm c}$ is the total correction factor.

| $S_i$ (Jy) | $S_f$ (Jy) | $S$ (Jy) | $\Delta S$ (Jy) | N | $C_{\rm fdr}$ | $C_{\rm c}$ | $V(S)$ (%) | $S^{2.5}\,dN/dS$ (Jy$^{3/2}$ sr$^{-1}$) |
|---|---|---|---|---|---|---|---|---|
| 0.020 | 0.032 | 0.026 | 0.0119 | 72 | 0.972 | $2.058^{+0.232}_{-0.129}$ | 17.08 | 724.60 ± 85.40 |
| 0.032 | 0.051 | 0.041 | 0.0189 | 88 | 0.977 | $1.450^{+0.114}_{-0.109}$ | 74.03 | 290.99 ± 31.02 |
| 0.051 | 0.081 | 0.066 | 0.0301 | 95 | 0.989 | $1.333^{+0.113}_{-0.105}$ | 98.37 | 442.51 ± 45.40 |
| 0.081 | 0.129 | 0.105 | 0.0479 | 102 | 1.000 | $1.272^{+0.094}_{-0.112}$ | 99.47 | 910.75 ± 90.18 |
| 0.129 | 0.205 | 0.167 | 0.0764 | 78 | 0.987 | $1.208^{+0.136}_{-0.083}$ | 99.98 | 1305.57 ± 147.83 |
| 0.205 | 0.327 | 0.266 | 0.1217 | 63 | 1.000 | $1.288^{+0.166}_{-0.159}$ | 100.00 | 2289.70 ± 288.47 |
| 0.327 | 0.521 | 0.424 | 0.1938 | 50 | 1.000 | $1.250^{+0.287}_{-0.183}$ | 100.00 | 3546.95 ± 501.61 |
| 0.521 | 0.829 | 0.675 | 0.3087 | 26 | 1.000 | $1.173^{+0.248}_{-0.213}$ | 100.00 | 3478.74 ± 682.24 |
| 0.829 | 1.321 | 1.075 | 0.4918 | 16 | 1.000 | $1.071^{+0.181}_{-0.167}$ | 100.00 | 3932.71 ± 983.18 |
| 1.321 | 2.104 | 1.713 | 0.7834 | 10 | 1.000 | $1.071^{+0.231}_{-0.214}$ | 100.00 | 4941.84 ± 1562.75 |
| 2.104 | 3.352 | 2.728 | 1.2479 | 5 | 1.000 | $1.074^{+0.212}_{-0.217}$ | 100.00 | 4980.67 ± 2227.42 |
| 3.352 | 5.340 | 4.346 | 1.9879 | 2 | 1.000 | $0.900^{+0.211}_{-0.212}$ | 100.00 | 3356.08 ± 2373.10 |
| 5.340 | 8.507 | 6.924 | 3.1667 | 1 | 1.000 | $0.800^{+0.200}_{-0.300}$ | 100.00 | 2998.93 ± 2998.93 |
| 8.507 | 13.551 | 11.029 | 5.0445 | 1 | 1.000 | $0.750^{+0.250}_{-0.250}$ | 100.00 | 5652.67 ± 5652.67 |
| 13.551 | 21.587 | 17.569 | 8.0358 | 1 | 1.000 | $0.732^{+0.268}_{-0.241}$ | 100.00 | 11094.44 ± 11094.44 |